Chinese Chemical Letters 33 (2022) 4264–4268

Contents lists available at ScienceDirect

Chinese Chemical Letters

journal homepage: www.elsevier.com/locate/cclet

Forrestiacids C and D, unprecedented triterpene-diterpene adducts from *Pseudotsuga forrestii*

Peng-Jun Zhou[a,b], Yi Zang[c], Cong Li[c], Lin Yuan[d], Huaqiang Zeng[e], Jia Li[c], Jin-Feng Hu[a,b,*], Juan Xiong[a,*]

[a] *Department of Natural Medicine, School of Pharmacy, Fudan University, Shanghai 201203, China*
[b] *School of Pharmaceutical Sciences, Zhejiang Provincial Key Laboratory of Plant Ecology and Conservation, Taizhou University, Taizhou 318000, China*
[c] *State Key Laboratory of Drug Research, Shanghai Institute of Materia Medica, Chinese Academy of Sciences, Shanghai 201203, China*
[d] *College of Chemistry and Bioengineering, Hunan University of Science and Engineering, Yongzhou 425199, China*
[e] *Frontier Research Center for Multidisciplinary Sciences, School of Chemistry and Chemical Engineering, Northwestern Polytechnical University, Xi'an 710072, China*

ARTICLE INFO

Article history:
Received 23 September 2021
Revised 20 November 2021
Accepted 6 December 2021
Available online 9 December 2021

Keywords:
Forrestiacid
Pseudotsuga forrestii
Pinaceae
Michael adduct
Lipogenesis inhibitor

ABSTRACT

Forrestiacids C (**1**) and D (**2**), a pair of C-25 epimeric triterpene–diterpene adducts were isolated from the needles and twigs of the vulnerable conifer *Pseudotsuga forrestii*. This unprecedented class of compounds might be generated *via* an intermolecular Michael addition reaction of a rearranged 6/6/5/5-fused spiro-lanostene with an abietene. Their structures were established by spectroscopic data and X-ray crystallography. The adducts showed inhibitory activities against the ATP-citrate lyase (ACL) and acetyl-CoA carboxylase 1 (ACC1), two rate-limiting enzymes in the *de novo* lipogenesis pathway.

Pinaceae, the largest conifer family with 220 to 250 species assigned to 11 genera and are distinctive in being primarily trees rather than shrubs [1]. Species of the Pinaceae are among the most valuable and commercially important plants (*e.g.*, cedar, fir, larch, pine, and spruce). This family has also attracted great interest for higher potential in the field of natural products drug discovery. A survey unveiled that Pinaceae ranked among the top-20 privileged drug-prolific families that produced high numbers of approved drugs [2].

Highly concerning is that 34% of the conifer species worldwide are currently threatened with extinction [3]. As for Pinaceae, there are 39 species recorded in the first volume of the China Plant Red Data Book (CPRDB). This signifies that this family occupies a great proportion (*ca.* 10%) of this reference, which listed a total of 388 species [4]. Plant diversity loss significantly exacerbates the complications in the discovery of new natural products-derived drugs owing to the rare and endangered plants (REPs) being better botanical sources [2,5,6]. An important goal for the conservation of the endangered plants is to provide key resources for researchers for new chemistry with utility in the control of new and emerging drug targets [7]. Thus, there is an urgent need to prioritize protection and utilization of these fragile plant species. In recent years, we have paid special attention to rare and endangered coniferous plants native to China [8]. In particular, REPs in the Pinaceae family have aroused an extra interest [9,10], due to their high potency in drug discovery, relatively other species diversity, and easier sample collections from the renewable needles and twigs from these large trees distributed and managed in the wild or cultivated in botanic gardens.

As a small genus in Pinaceae, *Pseudotsuga* comprises only a few recognized species distributed in the northern hemisphere, demonstrating a typical eastern Asia and western North America disjunct distribution patterns [4,11]. The type species *P. menziesii*, Douglas-fir, is one of the most economically important timbers in the world [11]. In China, there are five endemic *Pseudotsuga* species (*i.e.*, Asian Douglas-fir) or varieties: *P. forrestii*, *P. sinensis*, *P. brevifolia*, *P. gaussenii*, and *P. wilsoniana* [1]. All these species are recorded as vulnerable or endangered in CPRDB [4], and have also been nationally protected at the 'second-grade' in China [12].

The relict *Pseudotsuga* species *P. forrestii* is distributed within a total area of *ca.* 5000 km^2 (mainly in the Lancang river basin

* Corresponding authors at: Department of Natural Medicine, School of Pharmacy, Fudan University, Shanghai 201203, China.
E-mail addresses: jxiong@fudan.edu.cn (J. Xiong), jfhu@tzc.edu.cn, jfhu@fudan.edu.cn (J.-F. Hu).

https://doi.org/10.1016/j.cclet.2021.12.009
1001-8417/

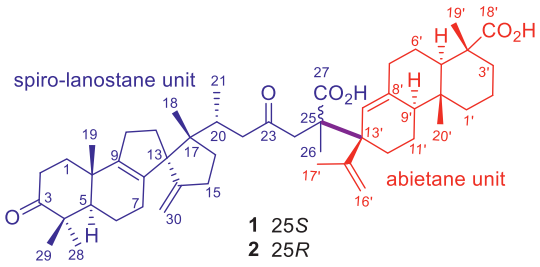

Fig. 1. A new class of terpenoid hetero-dimeric Michael adducts from *Pseudotsuga forrestii*.

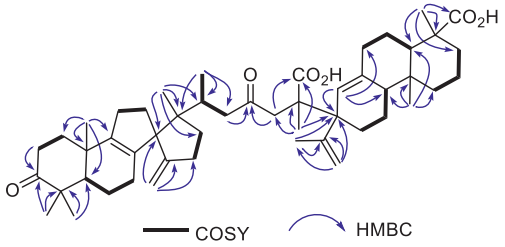

Fig. 2. COSY and key HMBC correlations of **1** and **2**.

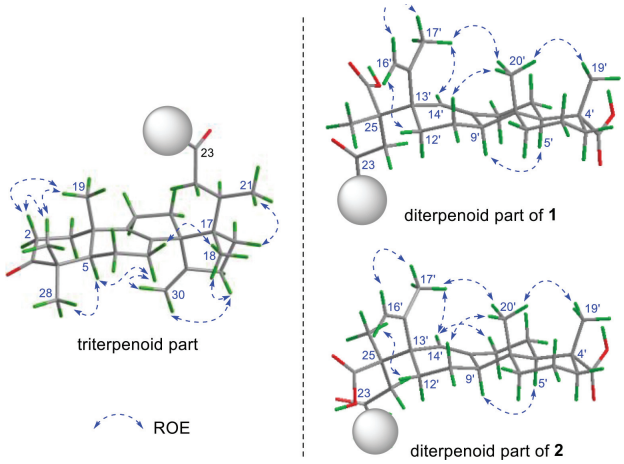

Fig. 3. ROE correlations of **1** and **2**.

and partly in the Jinsha river basin in south-western China) [1,4]. Besides timber, *P. forrestii* has a high ornamental value since its pinecones look like a blooming rose after ripening. In a preceding study on *P. forrestii*, two unique triterpene–diterpene adducts (forrestiacids A and B, *m/z* 769 $[M+H]^+$) featuring a novel carbon skeleton formed by intermolecular Diels-Alder cycloadditions between a spiro-lanostane triterpene unit and an abietadiene unit (Fig. S1 in Supporting information), were obtained by the implementation of HR-MS/MS-based molecular ion networking (MoIN) [13]. Further purification of the minor metabolites with the same target pseudo-molecular ion $[M+H]^+$ at *m/z* 769 by the guidance of MoIN (Fig. S2 in Supporting information) afforded another two unprecedented hetero-dimers (**1** and **2**) (Fig. 1), but constructed *via* an intermolecular Michael addition reaction of a rearranged 6/6/5/5-fused spiro-lanostene (C_{30}-unit) with an abietene (C_{20}-unit). The intriguing skeleton features a unique single C–C bond between C-25 (C_{30}-unit) and C-13′ (C_{20}-unit), which is quite different from those in the Diels-Alder adducts (forrestiacids A and B) [13]. Herein, we describe their isolation and structural elucidation, together with the lipogenesis inhibitory activities. This work is the Part XXI in a series of "Phytochemical and biological studies on rare and endangered plants endemic to China" (for Part XX, see ref. [13]).

Forrestiacid C (**1**), obtained as colorless needles from MeOH, was assigned the molecular formula $C_{50}H_{72}O_6$ as evidenced by the HR-ESI-MS ion at *m/z* 791.5194 $[M+Na]^+$ (calcd. for $C_{50}H_{72}O_6Na$, 791.5221). In the up-field region of the ^1H NMR spectrum of **1**, eight singlet methyls and one doublet methyl were observed at δ_H 0.82 (s, 3H), 0.88 (s, 3H), 0.98 (d, $J=6.5$ Hz, 3H), 1.17 (s, 3H), 1.20 (s, 6H), 1.43 (s, 3H), 1.73 (s, 3H), and 2.05 (s, 3H) (Table 1). Two pairs of olefinic proton resonances at δ_H 4.86/4.65 and 5.28/5.12 (each 1H, br s) arose from two exomethylene groups. The ^{13}C NMR data (Table 1) of **1**, with the aid of DEPT 135 and HSQC spectra, revealed 50 carbon resonances ascribable for nine methyls, 19 methylenes, five methines, 13 quaternary carbons, two carboxyls, and two ketocarbonyls. These data highlighted that **1** should be a ($C_{30}+C_{20}$) pentaterpene, similar to forrestiacids A and B [13].

Comprehensive analyses of the 1D and 2D NMR spectroscopic data of **1** implied the presence of a spiro-lanostane-type tetracyclic triterpenoid and an abietadiene-type diterpenoid unit (Fig. 2). For the triterpenoid part, the rearranged 6/6/5/5-fused spiro-lanostane nucleus bearing a 3-ketocarbonyl group (δ_C 216.0) and the double allyl nodal [*i.e.*, spiro[4.4]nona-8,14(30)-diene] motif was evidenced by the COSY and HMBC correlations as depicted in Fig. 2. As for the abietane part, an exomethylene group was located at C-15′ based on the HMBC correlations from H_2-16′ (δ_H 5.28/5.12) to C-15′/C-13′, and from H_3-17′ (δ_H 2.05) to C-13′/C-15′/C-17′ (Fig. 2). Another double bond, being a trisubstituted one [δ_H 6.36, s (H-14′); δ_C 138.6 (C-8′), 127.0 (C-14′)] was then elucidated to be sited between C-8′ and C-14′ by the HMBC correlations from H-14′ to C-7′, C-9′, and C-13′. In addition, the two carboxyl groups were assigned to attach to C-4′ and C-25, respectively, on the basis of HMBC cross peaks of H_3-19′ with C-4′ and C-18′ (δ_C 181.2), and of H_3-26 with C-25 and C-27 (δ_C 177.9). The remaining keto-carbonyl group at δ_C 209.6 was placed at C-23 based on its HMBC correlations with the two pairs of deshielded methylene protons of H_2-22 (δ_H 2.88/2.49) and H_2-24 (δ_H 3.60/2.89).

Moreover, the spiro-lanostane fragment was connected with the abietadiene by the formation of a new carbon–carbon single bond between C-25 and C-13′. This was defined by the HMBC correlations from H_3-26 (δ_H 1.73) to C-24, C-25, C-27, and C-13′.

Further inspection of the ROESY spectrum of **1** (Fig. 3) confirmed that the relative configuration of the spiro-lanostane nucleus was consistent with those of structurally related compounds, such as neoabiestrine F and forrestiacids A and B [13]. Concerning the abietene unit, its relative configuration could be readily assigned as shown in Fig. 3 based on the ROE correlations of H_3-19′/H_3-20′ and H-5′/H-9′. The isopropenyl group at C-13′ was β-positioned as evidenced by the diagnostic correlation between H_3–17′ and H_3–20′. However, determination of the stereochemistry at the quaternary carbon C-25 proved challenging due to the absence of available ROESY data for this flexible alkyl chain.

Interestingly, accompanied with **1**, its C-25 epimer, forrestiacid D (**2**), co-occurred in the same subfraction (for details, see Experimental in Supporting information). The molecular formula of **2** was determined to be identical with **1** from the positive-mode HR-ESI-MS ion at *m/z* 791.5213 $[M+Na]^+$ (calcd. 791.5221). Consistently, the ^1H and ^{13}C NMR spectroscopic data of **2** highly resembled those of **1** (Table 1). In terms of the ^{13}C chemical shifts, the largest difference between the two isolates was only 0.5 ppm (C-22, δ_C 46.3 *vs.* 45.8). It was similar with the ^1H NMR data—there were just two positions where the proton resonances differed by 0.2 and 0.3 ppm (*i.e.*, H-14′ and H-24b, respectively). The aforementioned data suggested that compound **2** should be a diastereoisomer of **1** with a different stereochemistry at C-25 and/or C-13′. This assumption was reinforced by further analyses of the ^1H–^1H COSY and HMBC spectra, which revealed that **2** did possess

Table 1
^{1}H (600 MHz) and ^{13}C (150 MHz) NMR data (δ in ppm, J in Hz, in pyridine-d_5) for **1** and **2**.

No.	**1**		**2**	
	δ_H	δ_C	δ_H	δ_C
Triterpenoid part (C_{30}-unit)				
1	α: 1.78, m	35.9	α: 1.74, m	35.9
	β: 2.32, m		β: 2.32, m	
2	α: 2.53, ddd (16.6, 8.0, 5.0)	34.8	α: 2.51, ddd (16.0, 7.2, 3.0)	34.4
	β: 2.66, ddd (16.6, 10.4, 7.5)		β: 2.64, ddd (16.0, 10.6, 7.3)	
3		216.0		216.0
4		47.3		47.3
5	1.73, br d (11.0)	51.2	1.73, dd (10.9, 3.6)	51.2
6	α: 1.70, m	20.8	α: 1.72, m	20.8
	β: 1.66, m		β: 1.64, m	
7	α: 1.98, m	26.7	α: 1.95, m	26.7
	β: 2.15, m		β: 2.11, m	
8		136.6		136.6
9		148.1		148.0
10		36.2		36.2
11	α: 1.98, m	26.8	α: 1.95, m	26.8
	β: 2.15, m		β: 2.12, m	
12	α: 2.09, m	32.9	α: 2.06, m	32.5
	β: 1.39, m		β: 1.36, m	
13		68.5		68.5
14		156.0		155.8
15	α: 2.32, m	27.5	α: 2.33, m	27.5
	β: 2.18, m		β: 2.23, m	
16	α: 1.58, m	38.0	α: 1.57, m	38.2
	β: 1.44, m		β: 1.42, m	
17		49.3		49.3
18	0.88, s	18.9	0.89, s	19.0
19	1.20, s	18.8	1.26, s	19.1
20	2.53, m	34.5	2.58, m	34.7
21	0.98, d (6.5)	16.4	0.99, d (6.5)	16.4
22	2.88, dd (17.4, 5.8)	46.3	2.98, br d (15.6)	45.8
	2.49, br d (17.4)		2.41, m	
23		209.6		209.5
24	3.60, d (16.2)	48.7	3.68, d (17.5)	48.5
	2.89, d (16.2)		2.59, d (17.5)	
25		50.1		49.9
26	1.73, s	18.9	1.79, s	19.0
27		177.9		177.8
28	1.20, s	26.7	1.19, s	26.7
29	1.17, s	21.3	1.19, s	21.4
30	4.86, br s; 4.65, br s	104.6	4.84, br s; 4.65, br s	104.5
Diterpenoid part (C_{20}-unit)				
1′	1.60, m; 1.09, m	38.4	1.59, m; 1.11, m	38.5
2′	1.45, m, 2H	18.5	1.52, m, 2H	18.5
3′	2.06, m; 1.78, m	37.7	2.08, m; 1.79, m	37.7
4′		47.3		47.3
5′	2.29, br d (11.4)	49.3	2.30, br d (11.6)	49.2
6′	2.00, m; 1.61, m	25.2	1.97, m; 1.62, m	25.2
7′	2.46, m; 1.57, m	35.7	2.44, m; 1.59, m	35.8
8′		138.6		138.6
9′	1.85, br d (ol.)	51.9	1.84, br d (10.0)	51.9
10′		38.2		38.2
11′	1.51, m; 1.42, m	19.5	1.51, m; 1.45, m	19.4
12′	2.20, m; 1.85, m	27.9	2.22, m; 1.82, m	28.1
13′		49.5		49.8
14′	6.36, s	127.0	6.16, s	126.9
15′		148.2		148.5
16′	5.28, br s; 5.12, br s	115.3	5.29, br s; 5.12, br s	115.4
17′	2.05, s	23.9	2.01, s	23.6
18′		181.2		181.2
19′	1.43, s	17.7	1.42, s	17.7
20′	0.82, s	14.9	0.80, s	15.0

the same 2D structure as **1**. Similar to **1**, a key correlation between H_3-17′ and H_3-20′ was also observed in the ROESY spectrum of **2**, assigning a same relative configuration at C-13′ in both **1** and **2**. Taken together, compound **2** was undoubtedly deduced to be a C-25 epimer of **1**.

Determination of the C-25 configurations in **1** and **2** was a difficult task. The electronic circular dichroism (ECD) spectra of the two epimers were overlaid with each other (Fig. S3 in Supporting information), precluding the application of ECD calculations. Moreover, the NMR shifts are very similar between **1** and **2**, just as described above. The NMR calculations would thus most likely not be able to differentiate between the two epimers. In our experience, NMR calculations commonly produce deviations from ^{13}C NMR experimental values of 1 ppm or more, so the error associated with the calculations are greater than the difference in the NMR shifts between the different epimers. As expected, the results

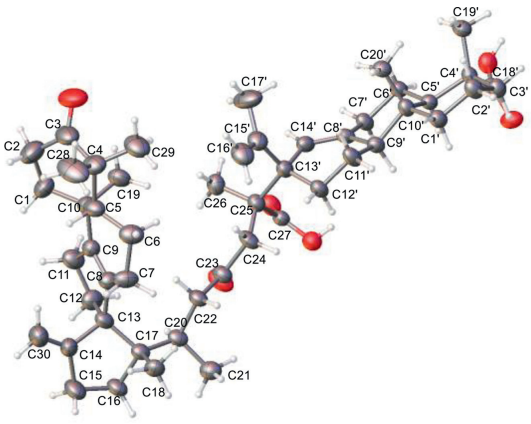

Fig. 4. OLEX2 drawing of compound **1** (more close-up views shown in Fig. S4 in Supporting information).

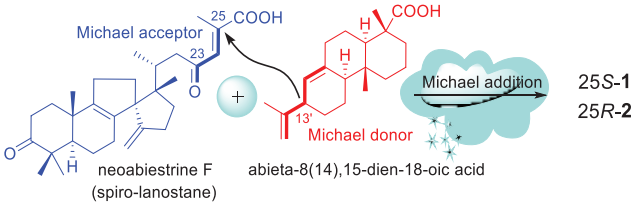

Scheme 1. Proposed biosynthetic pathway for **1** and **2**.

obtained from the preliminary GIAO NMR calculations with DP4+ probability analysis predicted that, the two epimers both matched closely with the calculated data of (25*S*)-isomer with 100% probability, along with 0% probability for the (25*R*)-isomer. Hence, in the case of **1** and **2**, the quantum NMR computational method also seems ineffectual and powerless. Actually, the limit of NMR calculations for the structural assignment of complex natural products has been well documented by Marcarino *et al.* [14].

Fortunately, after repeated attempts, a qualified crystal of **1** acquired in MeOH allowed a successful performance of single crystal X-ray diffraction [Flack parameter 0.02(18), Fig. 4]. This unambiguously confirmed the relative and absolute configurations of **1**, especially the configuration at C-25 (25*S*). The whole structure of (5*R*,10*S*,13*R*,17*S*,20*R*,25*S*,4′*R*,5′*R*,9′*S*,10′*R*,13′*S*)-**1**, was thus unequivocally established as depicted. Accordingly, the absolute configuration of **2** was defined as (5*R*,10*S*,13*R*,17*S*,20*R*,25*R*,4′*R*,5′*R*,9′*S*,10′*R*,13′*S*).

The structural features implied that **1** and **2** would be generated *via* a Michael addition between a unique spiro-lanostane-type triterpenoid precursor neoabiestrine F (co-occurring in the title plant [13]) and an abietadiene precursor (Scheme 1). The 24-en-23-one group in the side chain of neoabiestrine F would act as the 'Michael acceptor', whereas the diene motif in the diterpenoid would act as the 'Michael donor'.

Michael addition is one of the most important C–C bond-forming reactions in synthetic organic chemistry. The natural product biosynthetic machinery also uses a Michael-type addition to synthesize structurally diverse bioactive compounds [15]. So far, a number of naturally occurring Michael adducts (*e.g.*, polyketides [16a], cytochalasin homodimer [16b], trimeric macrodiolide [16c], and *ent*-kauranoid dimers [16d]) with interesting bioactivities have been reported. Among them, the terpenoid homo- or hetero-dimers are quite rare. To our knowledge, only a few have been encountered. For examples, three Michael adducts of *ent*-kaurane-type diterpenoid homo-dimers from the *Isodon* species [16d,e]. Forrestiacids C and D are the first two triterpene–diterpene adducts formed by Michael addition and represent an unusual chemical class of terpenoid hetero-dimers.

Table 2
Inhibitory activities of **1** and **2** against ACL and ACC1.

Compound	Inhibitory activity (IC_{50}) [a]	
	ACL	ACC1
1	10.99 ± 1.52 μmol/L	7.84 ± 0.06 μmol/L
2	22.78 ± 5.95 μmol/L	> 40 μmol/L
BMS 303141 [b]	0.46 ± 0.13 μmol/L	N.T.[d]
ND630 [c]	N.T.	2.30 ± 0.14 nmol/L

[a] The values indicate 50% ACL or ACC1 inhibitory effects. These data are expressed as the mean ± standard error of mean (SEM) of triplicate experiments.
[b] Positive control for the ACL assay.
[c] Positive control for the ACC1 assay.
[d] N.T.: Not tested.

The efficacy of bempedoic acid [the first ATP-citrate lyase (ACL) inhibitor approved by Food and Drug Administration (FDA)] as a low-density lipoprotein cholesterol (LDL-C)-lowering agent, has validated ACL inhibition as a therapeutic strategy for glycolipid metabolic disorders (*e.g.*, hyperlipidemia and hypercholesterolemia) [17,18]. In our previous study, forrestiacids A and B, the two [4 + 2]-adducts exhibited potent inhibitory effects against ACL, and elicited dual inhibition on the fatty acid and cholesterol syntheses in HepG2 cells [13]. Continuing our studies on the discovery of novel ACL and lipogenesis inhibitors from natural products, compounds **1** and **2** were evaluated for their ACL inhibitory effects. As illustrated in Table 2, they both displayed remarkable inhibition on ACL, with 50% inhibiting concentration (IC_{50}) values of 10.99 and 22.78 μmol/L, respectively. BMS 303141 was used as the positive control (IC_{50}: 0.46 ± 0.13 μmol/L). Interestingly, bempedoic acid and forrestiacids A–D all are dicarboxylic acid derivatives. Compared with the Diels-Alder adducts forrestiacids A and B (IC_{50}s < 5 μmol/L) [13], the Michael adducts (**1**, **2**), with the absence of a bridged-ring system (Fig. S1), showed relatively weaker inhibitory effects against ACL, although they have the same molecular weight. In addition, the 25*S*-isomer (**1**) demonstrated more potent inhibitory effect on ACL than its epimer (**2**). Interestingly, the 25*S*-isomer (**1**) also displayed significant inhibition (IC_{50}: 7.84 μmol/L) against acetyl-CoA carboxylase 1 (ACC1), which is also one of the rate-limiting enzymes in fatty acid synthesis by converting acetyl-CoA to malonyl CoA [19]. ACC1 has been considered as a potential drug target for glycolipid metabolic disorders (especially for hepatic steatosis). It is worth mentioning that, only slight inhibitory effects on ACL and ACC1 were found for the triterpene precursor neoabiestrine F, with IC_{50} values of 24.33 and 24.40 μmol/L, respectively. Taken together, the above findings indicated that the chirality of C-25 in forrestiacids C and D might play an important role in the lipogenesis inhibition of these Michael adducts, which warrants further investigations.

Declaration of competing interest

The authors declare that they have no known competing financial interests or personal relationships that could have appeared to influence the work reported in this paper.

Acknowledgments

This work was supported by grants from the National Natural Science Foundation of China (Nos. 21937002, 81773599, 21772025). The authors thank Prof. Mark T. Hamann (Medical University of South Carolina, USA) and Dr. Yike Zou (Department of Chemistry and Biochemistry, University of California, at Los Angeles, USA) for their kind suggestions and assistance with the NMR quantum computations.

Supplementary materials

Supplementary material associated with this article can be found, in the online version, at doi:10.1016/j.cclet.2021.12.009.

References

[1] (a) L.K. Fu, N. Li, R.R. Mill, Z.Y. Wu, P.H. Raven, Flora of China, 4, Science Press (Beijing) & Missouri Botanical Garden Press (St. Louis), 1999, pp. 11–52;
(b) The Plant List, Version 1.1, A Working List for All Plant Species, The Plant List, 2013. http://www.theplantlist.org /1.1/browse/G/Pinaceae/.
[2] F. Zhu, C. Qin, L. Tao, et al., Proc. Natl. Acad. Sci. U. S. A. 108 (2011) 12943–12948.
[3] The IUCN Red List of Threatened Species, Version 2021-3. https://www.iucnredlist.org.
[4] L.K. Fu, J.M. Jin, China Plant Red Data Book. Rare and Endangered Plants I, Science Press, Beijing and New York, 1992.
[5] M.A. Ibrahim, M. Na, J. Oh, et al., Proc. Natl. Acad. Sci. U. S. A. 110 (2013) 16832–16837.
[6] S.H.M. Butchart, M. Walpole, B. Collen, et al., Science 328 (2010) 1164–1168.
[7] J.L. Fox, Science 226 (1984) 150.
[8] G.L. Ma, N. Guo, X.L. Wang, et al., Bioorg. Chem. 105 (2020) 104445.
[9] W. Jiang, J. Xiong, Y. Zang, et al., Phytochemistry 169 (2020) 112161.
[10] T. Huang, S.H. Ying, J.Y. Li, et al., Phytochemistry 169 (2020) 112184.
[11] X.X. Wei, Z.Y. Yang, Y. Li, et al., Mol. Phylogenet. Evol. 55 (2010) 776–785.
[12] National Forestry and Grassland Administration. List of National Key Protected Wild Plants 2021, http://www.gov.cn/zhengce/zhengceku/2021-09/09/content_5636409.htm.
[13] J. Xiong, P.J. Zhou, H.W. Jiang, et al., Angew. Chem. Int. Ed. 60 (2021) 22270–22275.
[14] M.O. Marcarino, S. Cicetti, M.M. Zanardi, et al., Nat. Prod. Rep. 39 (2022) 58–76.
[15] (a) A. Michael, J. Prakt. Chem. 35 (1886) 349–356;
(b) P. Perlmutter, Conjugate Addition Reactions in Organic Synthesis, Pergamon Press, Oxford, 1992.
[16] (a) A. Miyanaga, Nat. Prod. Rep. 36 (2019) 531–547;
(b) Z. Wu, X. Zhang, C. Chen, et al., Org. Lett. 22 (2020) 2162–2166;
(c) T.T. Wang, Y.J. Wei, H.M. Ge, et al., Org. Lett. 20 (2018) 2490–2493;
(d) H.B. Zhang, J.X. Pu, Y. Zhao, et al., Tetrahedron Lett. 52 (2011) 6061–6066;
(e) Y. Zhao, S.X. Huang, W.L. Xiao, et al., Tetrahedron Lett. 50 (2009) 2019–2023.
[17] (a) K.H.G. Verschueren, C. Blanchet, J. Felix, et al., Nature 568 (2019) 571–575;
(b) K.E. Wellen, G. Hatzivassiliou, U.M. Sachdeva, et al., Science 324 (2009) 1076–1080.
[18] (a) K.K. Ray, H.E. Bays, A.L. Catapano, et al., N. Engl. J. Med. 380 (2019) 1022–1032;
(b) S.L. Pinkosky, R.S. Newton, E.A. Day, et al., Nat. Commun. 7 (2016) 13457.
[19] M. Hunkeler, A. Hagmann, E. Stuttfeld, et al., Nature 558 (2018) 470–474.